Polarization and Interference Effects in Ionization of Li by Ion Impact

R. Hubele,[1] A. LaForge,[1] M. Schulz,[2,3] J. Goullon,[1] X. Wang,[1,4] B. Najjari,[1] N. Ferreira,[1] M. Grieser,[1] V. L. B. de Jesus,[5]
R. Moshammer,[1] K. Schneider,[1] A. B. Voitkiv,[1,6] and D. Fischer[1,*]

[1]*Max Planck Institute for Nuclear Physics, Saupfercheckweg 1, 69117 Heidelberg, Germany*
[2]*Physics Department and LAMOR, Missouri University of Science and Technology, Rolla, Missouri 65409, USA*
[3]*Institut für Kernphysik, Universität Frankfurt, Max-von-Laue Strasse 1, 60438 Frankfurt, Germany*
[4]*Shanghai EBIT Laboratory, Institute of Modern Physics, Fudan University, Shanghai 200433, China*
[5]*Instituto Federal de Educação, Ciência e Tecnologia do Rio de Janeiro (IFRJ),*
Rua Lucio Tavares 1045, 26530-060 Nilópolis, Rio de Janeiro, Brazil
[6]*Extreme Matter Institute EMMI, GSI Helmholtzzentrum für Schwerionenforschung GmbH, Planckstrasse 1,*
64291 Darmstadt, Germany

We present initial-state selective fully differential cross sections for ionization of lithium by 24 MeV O^{8+} impact. The data for ionization from the $2s$ and $2p$ states look qualitatively different from each other and from $1s$ ionization of He. For ionization from the $2p$ state, to which in our study the $m_L = -1$ substate predominantly contributes, we observe orientational dichroism and for $2s$ ionization pronounced interference which we trace back to the nodal structure of the initial-state wave function.

With rapidly increasing computer power theoretical models are often capable of at least qualitatively describing and even predicting properties of very complex and exotic systems involving a large number of interacting particles (e.g., Ref. [1]). One might thus suspect that relatively simple systems, containing only a few bodies, like, e.g., a structureless particle colliding with a light atom, do not represent a serious challenge to theory anymore. Indeed, measured total cross sections and differential ejected electron spectra for various processes occurring in such collisions can often be calculated with a high degree of accuracy (e.g., Refs. [2–4]). However, this seemingly gratifying situation emerges as increasingly sobering as more detailed measurements are performed.

One big advantage of studying simple systems is that experiments, in which the complete kinematic information about every single particle in the system is obtained, are feasible (for reviews see, e.g., Refs. [5–8]). The fully differential cross sections (FDCS) that can be extracted from such measurements offer a very sensitive test of theoretical models. For atomic ionization by electron impact the first kinematically complete experiment was performed more than four decades ago [9]. But it took another three decades before theoretical developments resulted in a satisfactory description of experimental data for the simplest target atoms (e.g., Refs. [10,11]).

Fully differential studies of ion impact ionization are much more challenging, from both an experimental and a theoretical point of view, because of the much larger projectile mass compared to electrons. Only after reaction microscopes (ReMi) [7,8] were developed the first kinematically complete experiments for ion impact ionization were performed (e.g., Refs. [6,12–14]). Even for small

perturbation parameters η (projectile charge to speed ratio), for which the ionization dynamics was believed to be essentially understood, significant discrepancies were found between experiment and theory [13] which persist until today although elaborate nonperturbative models have been developed [15]. For large η, not even qualitative agreement could be achieved in spite of numerous and valuable theoretical efforts (e.g., Refs. [16–18]).

In particular, the discrepancies at small η were very surprising and vividly debated over the past years (e.g., Refs. [15,19–25]). A promising explanation towards resolving this puzzle was eventually proposed by Egodapitiya *et al.* [26] and supported by Wang *et al.* [27]. Their experimental observations suggest an impact of the projectile coherence properties on the scattering process that is not considered in the available quantum-mechanical models. However, it is not clear that the severe discrepancies observed for large η can entirely be associated with the projectile coherence. It should further be noted that relatively little is known about the ionization dynamics for states other than $1s$ because all earlier experimental FDCS for ion impact have been obtained for the ground state of He. Though the sensitivity of low-energy electron emission on the electron initial momentum distribution has been reported for neon and argon targets [4], in these experiments it was not possible to resolve the actual initial state of the ionized electron. In this respect, alkali metals represent particularly attractive target systems. Because of the large difference in the binding energies of the single valence electron and the core electrons, the ionization process proceeds almost exclusively through the emission from the outer shell. However, until very recently only differential electron

spectra were reported [28,29] and today one data set is available on double differential cross sections as a function of scattering angle and electron energy [30]. In the latter study some qualitative differences for ionization of lithium from the $2s$ and $2p$ states were found.

In this Letter we report on FDCS for ionization of laser-cooled Li by ion impact. The results represent a major advancement with regard to two aspects. First, initial-state selective FDCS are accessible for the ionization of the $2s$ and $2p$ states because the target can be excited before the collision using a laser, where the $2p$ state was even polarized. Second, due to a substantially improved resolution compared to all earlier experiments obtaining FDCS, subtle features in the momentum distributions can be examined in unprecedented detail. The experiment became possible using a newly developed MOTReMi apparatus [31], i.e., a combination of a magneto-optical trap (MOT) with an electron recoil-ion momentum spectrometer. Qualitatively new features, not observed for $1s$ ionization of He, are found in the electron ejection angle dependence of the FDCS.

The experiment was performed at the test storage ring in Heidelberg. The setup has been described in some detail earlier [31], and only the salient points will be repeated here. A pulsed 24 MeV O^{8+} beam with a size of about 1 mm passed through a laser-cooled Li target in a MOT, which is part of the MOTReMi apparatus. The electrons and recoil ions produced in the collision were extracted towards two-dimensional position-sensitive channel plate detectors by a weak electric field of about 0.6 V/cm directed at an angle of 8° with respect to the projectile beam axis. A uniform magnetic field of 7.7 G, parallel to the extraction field, forced the electrons into cyclotron motion so that all electrons with transverse momenta of less than 1.3 a.u. hit the detector. Both detectors were set in coincidence, where a fast signal from the projectile buncher served as a time reference. The magnetic trapping field of the MOT was momentarily turned off for an undisturbed extraction and detection of the target fragments.

From the position information the electron and recoil-ion momentum components in the plane perpendicular to the extraction field could be determined. The third momentum component for both particles, parallel to the extraction field, was obtained from the time of flight from the collision region to the respective detector, which is contained in the coincidence time. The target temperature is about 2–3 orders of magnitude smaller than in a conventional ReMi apparatus and is thus no longer the main contributor to the recoil-ion momentum resolution. Instead, the resolution in the plane perpendicular to the extraction field of ± 0.05 a.u. is mainly due to the size of the reaction volume and in the direction of the extraction field (± 0.03 a.u.) due to the time structure of the projectile pulses. For the electron, the corresponding values are ± 0.05 and ± 0.01 a.u., respectively.

During the operation of the cooling lasers the initial Li valence state is not a pure $2s$ state, but a $2p$ population of about 20% was estimated [30]. In order to obtain data for pure $2s$ ionization, the lasers were turned off for 200 μs in the 1.3 ms period with no magnetic trapping field in each cycle. $2p$ ionization data were obtained by subtracting the number of "laser off" events from the number of "laser on" events. We further know that the $2p$ electrons predominantly populate the $m_L = -1$ state. In order for the lasers to have a trapping effect on the Li atoms, the light needs to be redshifted relative to the transition frequency. At the same time, the uniform magnetic field used to guide the electrons onto the detector leads to a Zeeman splitting such that this redshift minimizes for transitions to $2^2 P_{3/2}$ sublevels with large contributions of $m_L = -1$. Measuring the degree of polarization of the fluorescence light emitted from the target in different directions, we obtain the relative contributions of σ^-, π, and σ^+ transitions which directly reflect the m_L distribution in the excited state. This way we estimate a contribution of $m_L = -1$ and $m_L = 0$ of about 70% and 30%, respectively.

For the presentation of the FDCS we choose a coordinate system which is linked to the scattering plane spanned by the momentum transfer from the projectile to the target atom $\mathbf{q}$ and by the initial projectile momentum $\mathbf{p_0}$. The polar angle for the ejected electron momentum ϑ_{el} is measured with respect to the initial projectile beam axis. The azimuthal angle φ_{el} is measured in the plane perpendicular to the beam axis, i.e., in the azimuthal plane. $\varphi_{el} = $ 90° and 270° coincide with the direction of the transverse components of $\mathbf{q}$ and $-\mathbf{q}$, respectively. In Fig. 1 we present three-dimensional fully differential angular distributions of the ejected electrons for the ionization from the $2p$ (top) and $2s$ state (bottom). Here, the electron energy is fixed at 1.5 ± 0.5 eV and q at 0.3 ± 0.1 a.u. and 1.0 ± 0.2 a.u. for the $2p$ and $2s$ ionization, respectively.

For ionization of He in the ground state by ion or electron impact, typically a double lobe structure, with the so-called binary peak approximately in the direction of $\mathbf{q}$ and the recoil peak in the direction of $-\mathbf{q}$, is observed (e.g., Refs. [5,6]). Furthermore, the FDCS exhibit strict mirror symmetry relative to the scattering plane. For ionization of Li we also find a pronounced binary peak, but the recoil peak is completely absent. This is not surprising and can be explained by the small ionization potential. However, there are two features which make the present data for $2s$ and $2p$ ionization qualitatively different from each other and from He ionization. First, in the case of $2s$ ionization we observe side maxima to the binary peak in the azimuthal plane which are not seen for the $2p$ state. This feature is also present for smaller q (e.g., for $q = $ 0.3 a.u.), but it is less pronounced. Second, while for the $2s$ state the mirror symmetry with respect to the scattering plane is maintained (for all q), it appears to be broken for the $2p$ state. Both effects are most prominent in the
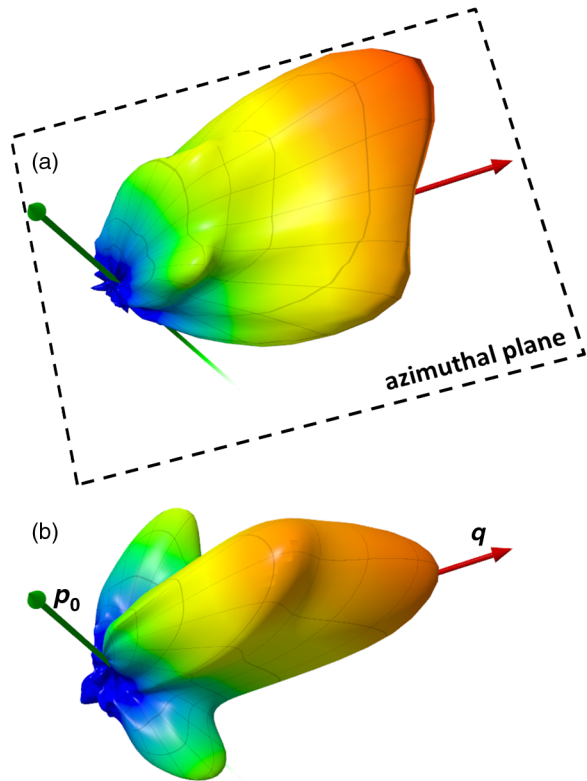
FIG. 1 (color online). Three-dimensional, fully differential angular distributions of electrons ejected from the (a) $2p$ and (b) $2s$ state of Li by 24 MeV O^{8+} impact. The electron energy is fixed at 1.5 eV and q at 0.3 a.u. for the $2p$ state and at 1.0 a.u. for the $2s$ state.
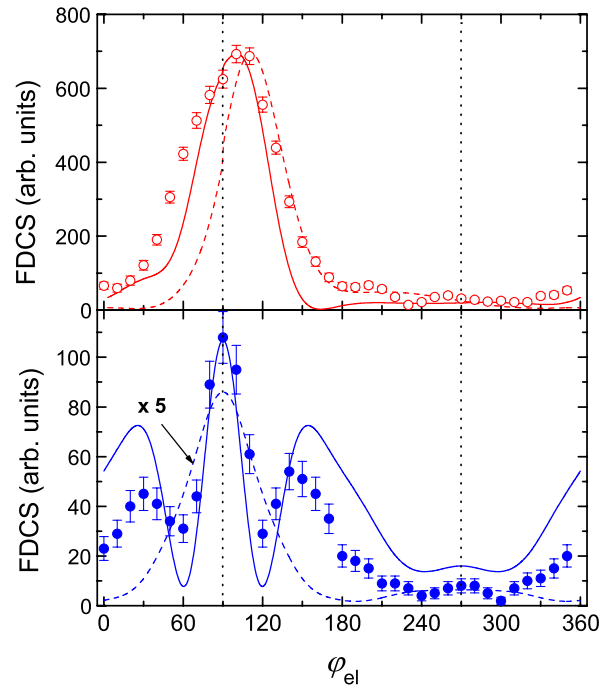

FIG. 2 (color online). Cut through the azimuthal plane of the FDCS shown in Fig. 1 for the $2p$ (open red symbols) and $2s$ states (solid blue symbols). Dashed curves, CDW-EIS calculations; solid curve, CDW-EIS-NN calculations. For explanation of theoretical models, see text.

azimuthal plane. In the following, we therefore discuss the FDCS for a cut along the azimuthal plane, which are shown in Fig. 2, in more detail.

First, we analyze the mirror symmetry properties with respect to the scattering plane (indicated by the vertical dotted lines at $\varphi_{el} = 90°$ and $270°$ in Fig. 2). The breaking of this symmetry in the $2p$ data (top panel), seen already in Fig. 1, becomes more evident in the direct comparison with the $2s$ data (bottom panel), which are perfectly symmetric. The $2p$ angular distribution is shifted relative to the $2s$ distribution, and therefore to the symmetry axis, by about 15°. This asymmetry is due to the polarization of the initial target state, i.e., the predominant population of the $m_L = -1$ substate. For a spherically symmetric initial state, i.e., when no magnetic substate is selected, spatial directions are only tagged by $\mathbf{p_0}$ and $\mathbf{q}$. The FDCS can thus only depend on the relative angles of the electron momentum to these vectors; i.e., they must satisfy the mirror symmetry with respect to the scattering plane mentioned above. The breaking of this symmetry by the target polarization is known as orientational dichroism and it has been observed in electron impact ionization of polarized sodium [32].

The dichroism is also predicted by a continuum distorted wave–eikonal initial state (CDW-EIS) calculation [33], which is shown as the dashed curve in Fig. 2. Here, the

interaction between the nuclei of the collision partners (NN interaction) is not accounted for. The initial electron population in the target was assumed to be 30% in the $m_L = 0$ state and 70% in the $m_L = -1$ state. The $m_L = 0$ contribution tends to "wash out" the dichroism, but nevertheless it is still clearly visible in the calculation and even more pronounced than in the experimental data. Better agreement with the measured FDCS is obtained when the NN interaction is included. This calculation, which we dub CDW-EIS-NN and which accounts for the interaction between the nuclei within the eikonal approximation [33], is shown as the solid curve in Fig. 2. The shift of the binary peak position from the symmetry axis in the data is now well reproduced by theory. This shows that the NN interaction has a tendency to reduce dichroism. The difference in the width of the peak between the measured and calculated FDCS is consistent with the experimental resolution, as we verified by convoluting the theoretical cross sections using the Monte Carlo method of Dürr *et al.* [34].

In the FDCS for ionization from the $2s$ state at $q = 1.0$ a.u., a splitting of the binary peak into a triple peak structure is clearly visible. Again, the dashed and solid curves represent CDW-EIS and CDW-EIS-NN calculations, respectively. Without the NN interaction the satellite peaks are completely absent in the theoretical FDCS, which are in rather poor agreement with the experimental data. In contrast, very nice qualitative agreement is achieved when the NN interaction is included in the

calculation and a pronounced triple peak structure is clearly visible. On the other hand, some quantitative discrepancies remain. In the following we will discuss what may cause the satellite peak structure seen in both theory and experiment.

First, we note that one major qualitative difference between a $2s$ and a $2p$ state, for which no satellite peaks are observed in the FDCS (at any q), is that the radial part of the wave function has a node for the $2s$ but not for the $2p$ state. Multiple peak structures in the FDCS have been observed for ionization of heavier atoms by electron impact from states with nodal structures in the wave function (e.g., Ref. [35]). An influence of the nodal structure on double differential electron angular distributions for $2s$ ionization of Li by heavy ion impact has also been discussed [28], but there no multiple peak structures were observed.

Useful information on potential effects of the nodal structure of the wave function on the FDCS for the present case can be obtained from a comparison between the CDW-EIS and CDW-EIS-NN calculations. If the satellite peak structures were entirely due to the nodal structure, they should be seen even if the NN interaction was not included in the calculation. In fact, they should become most pronounced in first-order calculations like the first Born approximation, where the characteristics of the initial state are not distorted by any higher-order effects. Instead, the multiple peak structure is completely absent in both the first Born approximation (not shown in Fig. 2) and the CDW-EIS calculation. It thus seems clear that the nodal structure alone cannot explain the features seen in the data. It is equally obvious that the NN interaction plays an essential role since only when it is incorporated in the calculation is the multiple peak structure present. On the other hand, the NN interaction alone, without consideration for the initial state, cannot explain the data either. We performed a test calculation for ionization of Li using a wave function with the nodal structure of the $1s$ state, but the binding energy of the $2s$ state, and here, no satellite maxima were found. In the following we will therefore attempt to explain the data by considering the initial state in conjunction with the NN interaction.

The $2s$ wave function has two maxima in coordinate space, a very small maximum at about 0.3 a.u., which contains only less than 2% of the total flux, and a significantly broader main maximum near 3 a.u. [36]. A minimum separating the two peaks occurs at about 0.8 a.u. In order to see the signature of the initial state's nodal structure, both maxima of the electron density have to contribute significantly to the transition amplitude. However, in the semiclassical impact parameter picture, the overall cross section is dominated by distant collisions (impact parameters $b \gtrsim 1$ a.u.) and the influence of the small inner maximum of the electron density is in most cases negligible. Only for small impact parameters

(as small as $b \sim 0.3$ a.u.) the effect of the nodal structure becomes observable in the FDCS.

If the NN interaction is ignored, as it is in the CDW-EIS calculation, no momentum is transferred from the projectile to the recoil ion, and the projectile momentum change is solely caused by the interaction with the electron. Under these conditions, there is only a weak correlation between the momentum transfer and the impact parameter, and it is not possible to select kinematic settings for which the impact parameters of the collisions are very small. This changes drastically if the NN interaction is included, i.e., in the CDW-EIS-NN model. Here the momentum transfer from the projectile to the target core correlates strongly with the impact parameter, and the momentum exchange becomes larger for smaller b. Hence, small impact parameters can be selected by choosing conditions where the momentum transfer $\mathbf{q}$ is essentially determined by the recoil-ion momentum, i.e., when $\mathbf{q}$ is significantly larger than the final electron momentum $\mathbf{p}_{el}$. Therefore, for $q = 1.0$ a.u. and $E_{el} = 1.5$ eV, one might expect the nodal structure of the wave function to lead to satellite peak structures which should be weaker at small q. This is indeed observed in the CDW-EIS-NN calculation and in the data.

In general, satellite structures can also be interpreted in terms of interference between two contributions to the transition amplitude, one associated with the inner and one with the outer part of the wave function. Such interference, in turn, can only occur if the incoming projectile wave covers both parts of the electron wave function coherently and, therefore, it is dependent on the projectiles coherence properties. Such dependence has been observed recently by Wang et al. [27] in FDCS in ion-helium collisions. There, differences between data taken with a coherent and an incoherent projectile beam have been explained by interference between amplitudes with and without the NN interaction. As pointed out by Wang et al., the interference is only observable if the transverse coherence length Δx is larger than the difference between the impact parameters Δb which mostly contribute to the interfering amplitudes.

In our experiment the quantitative discrepancies between theory and experiment may be related to the projectile coherence. In comparison to theory it looks like the interference structure seen in the calculation is partly blurred in the data. This is an effect which in principle could be caused by the experimental resolution. However, convoluting theory with the resolution by our Monte Carlo method [22,34] leads to no substantial change in the FDCS. On the other hand, a similar effect is also caused by a projectile beam which is not fully, but only partly, coherent. Overall, the data are satisfactorily described by theory.

In summary, we have presented fully differential ionization cross sections initial-state selectively. The data for $2s$ and $2p$ ionization look qualitatively different from each

other and from $1s$ ionization of He. In the $2p$ case the $m_L = -1$ substate is mostly populated, and this selection leads to orientational dichroism in the azimuthal dependence of the FDCS. In the FDCS for $2s$ ionization we observe a clear oscillating pattern which we ascribe to the nodal structure of the initial-state wave function. Compared to earlier measured data for ionization of helium, in the present study a remarkable qualitative agreement between theory and experiment has been achieved.

---

*fischer@mpi-hd.mpg.de

[1] C. H. Greene, A. S. Dickinson, and H. R. Sadeghpour, Phys. Rev. Lett. **85**, 2458 (2000).

[2] D. Belkić, I. Mančev, and J. Hanssen, Rev. Mod. Phys. **80**, 249 (2008).

[3] M. E. Rudd, Y. K. Kim, D. H. Madison, and J. W. Gallagher, Rev. Mod. Phys. **57**, 965 (1985).

[4] R. Moshammer, P. D. Fainstein, M. Schulz, W. Schmitt, H. Kollmus, R. Mann, S. Hagmann, and J. Ullrich, Phys. Rev. Lett. **83**, 4721 (1999).

[5] H. Ehrhardt, K. Jung, G. Knoth, and P. Schlemmer, Z. Phys. D **1**, 3 (1986).

[6] M. Schulz and D. H. Madison, Int. J. Mod. Phys. A **21**, 3649 (2006).

[7] R. Dörner, V. Mergel, O. Jagutzki, L. Spielberger, J. Ullrich, R. Moshammer, and H. Schmidt-Böcking, Phys. Rep. **330**, 95 (2000).

[8] J. Ullrich, R. Moshammer, A. Dorn, R. Dörner, L. P. H. Schmidt, and H. Schmidt-Böcking, Rep. Prog. Phys. **66**, 1463 (2003).

[9] H. Ehrhardt, M. Schulz, T. Tekaat, and K. Willmann, Phys. Rev. Lett. **22**, 89 (1969).

[10] T. N. Rescigno, M. Baertschy, W. A. Isaacs, and C. W. McCurdy, Science **286**, 2474 (1999).

[11] I. Bray, Phys. Rev. Lett. **89**, 273201 (2002).

[12] T. Weber, K. Khayyat, R. Dörner, V. Mergel, O. Jagutzki, L. Schmidt, F. Afaneh, A. Gonzalez, C. L. Cocke, A. L. Landers, and H. Schmidt-Böcking, J. Phys. B **33**, 3331 (2000).

[13] M. Schulz, R. Moshammer, D. Fischer, H. Kollmus, D. Madison, S. Jones, and J. Ullrich, Nature (London) **422**, 48 (2003).

[14] N. V. Maydanyuk, A. Hasan, M. Foster, B. Tooke, E. Nanni, D. H. Madison, and M. Schulz, Phys. Rev. Lett. **94**, 243201 (2005).

[15] M. McGovern, C. T. Whelan, and H. R. J. Walters, Phys. Rev. A **82**, 032702 (2010).

[16] M. Schulz, R. Moshammer, A. N. Perumal, and J. Ullrich, J. Phys. B **35**, L161 (2002).

[17] M. McGovern, D. Assafrão, J. R. Mohallem, C. T. Whelan, and H. R. J. Walters, Phys. Rev. A **81**, 042704 (2010).

[18] J. Fiol and R. E. Olson, J. Phys. B **37**, 3947 (2004).

[19] A. B. Voitkiv, B. Najjari, and J. Ullrich, J. Phys. B **36**, 2591 (2003).

[20] M. Foster, J. L. Peacher, M. Schulz, D. H. Madison, Z. Chen, and H. R. J. Walters, Phys. Rev. Lett. **97**, 093202 (2006).

[21] J. Fiol, S. Otranto, and R. E. Olson, J. Phys. B **39**, L285 (2006).

[22] M. Schulz, M. Dürr, B. Najjari, R. Moshammer, and J. Ullrich, Phys. Rev. A **76**, 032712 (2007).

[23] J. Colgan, M. S. Pindzola, F. Robicheaux, and M. F. Ciappina, J. Phys. B **44**, 175205 (2011).

[24] I. B. Abdurakhmanov, I. Bray, D. V. Fursa, A. S. Kadyrov, and A. T. Stelbovics, Phys. Rev. A **86**, 034701 (2012).

[25] K. A. Kouzakov, S. A. Zaytsev, Y. V. Popov, and M. Takahashi, Phys. Rev. A **86**, 032710 (2012).

[26] K. N. Egodapitiya, S. Sharma, A. Hasan, A. C. Laforge, D. H. Madison, R. Moshammer, and M. Schulz, Phys. Rev. Lett. **106**, 153202 (2011).

[27] X. Wang, K. Schneider, A. LaForge, A. Kelkar, M. Grieser, R. Moshammer, J. Ullrich, M. Schulz, and D. Fischer, J. Phys. B **45**, 211001 (2012).

[28] N. Stolterfoht, J.-Y. Chesnel, M. Grether, B. Skogvall, F. Frémont, D. Lecler, D. Hennecart, X. Husson, J. P. Grandin, B. Sulik, L. Gulyás, and J. A. Tanis, Phys. Rev. Lett. **80**, 4649 (1998).

[29] J. A. Tanis, J.-Y. Chesnel, F. Frémont, D. Hennecart, X. Husson, A. Cassimi, J. P. Grandin, B. Skogvall, B. Sulik, J.-H. Bremer, and N. Stolterfoht, Phys. Rev. Lett. **83**, 1131 (1999).

[30] A. C. LaForge, R. Hubele, J. Goullon, X. Wang, K. Schneider, V. L. B. de Jesus, B. Najjari, A. B. Voitkiv, M. Grieser, M. Schulz, and D. Fischer, J. Phys. B **46**, 031001 (2013).

[31] D. Fischer, D. Globig, J. Goullon, M. Grieser, R. Hubele, V. L. B. de Jesus, A. Kelkar, A. LaForge, H. Lindenblatt, D. Misra, B. Najjari, K. Schneider, M. Schulz, M. Sell, and X. Wang, Phys. Rev. Lett. **109**, 113202 (2012).

[32] A. Dorn, A. Elliott, J. Lower, E. Weigold, J. Berakdar, A. Engelns, and H. Klar, Phys. Rev. Lett. **80**, 257 (1998).

[33] D. Fischer, R. Moshammer, M. Schulz, A. Voitkiv, and J. Ullrich, J. Phys. B **36**, 3555 (2003).

[34] M. Dürr, B. Najjari, M. Schulz, A. Dorn, R. Moshammer, A. B. Voitkiv, and J. Ullrich, Phys. Rev. A **75**, 062708 (2007).

[35] M. A. Stevenson, L. R. Hargreaves, B. Lohmann, I. Bray, D. V. Fursa, K. Bartschat, and A. Kheifets, Phys. Rev. A **79**, 012709 (2009).

[36] R. D. Cowan, *The Theory of Atomic Structure and Spectra* (University of California Press, Berkeley, 1981).